

4. DIFFUSE SCATTERING AND RELATED TOPICS

1986), it is only recently that X-ray scattering techniques have been applied to this problem. In one form or another, all of the techniques for obtaining surface specificity in an X-ray measurement make use of the fact that the average interaction between X-rays and materials can be treated by the introduction of a dielectric constant $\varepsilon \approx 1 - (4\pi\rho e^2/m\omega^2) = 1 - \rho r_e \lambda^2/\pi$, where ρ is the electron density, r_e is the classical radius of the electron, and ω and λ are the angular frequency and the wavelength of the X-ray. Since $\varepsilon < 1$, X-rays that are incident at a small angle to the surface θ_0 will be refracted in the material toward a smaller angle $\theta_T \approx (\theta_0^2 - \theta_c^2)^{1/2}$, where the ‘critical angle’ $\theta_c \approx (\rho r_e \lambda^2/\pi)^{1/2} \approx 0.003$ rad ($\approx 0.2^\circ$) for most liquid crystals (Warren, 1968). Although this is a small angle, it is at least two orders of magnitude larger than the practical angular resolution available in modern X-ray spectrometers (Als-Nielsen *et al.*, 1982; Pershan & Als-Nielsen, 1984; Pershan *et al.*, 1987). One can demonstrate that for many conditions the specular reflection $R(\theta_0)$ is given by

$$R(\theta_0) \approx R_F(\theta_0) |\rho^{-1} \int dz \exp(-iQz) \langle \partial\rho/\partial z \rangle|^2,$$

where $Q \equiv (4\pi/\lambda) \sin(\theta_0)$, $\langle \partial\rho/\partial z \rangle$ is the normal derivative of the electron density averaged over a region in the surface that is defined by the coherence area of the incident X-ray, and

$$R_F(\theta_0) \approx \left(\frac{\theta_0 - \sqrt{\theta_0^2 - \theta_c^2}}{\theta_0 + \sqrt{\theta_0^2 - \theta_c^2}} \right)^2$$

is the Fresnel reflection law that is calculated from classical optics for a flat interface between the vacuum and a material of dielectric constraint ε . Since the condition for specular reflection, that the incident and scattered angles are equal and in the same plane, requires that the scattering vector $\mathbf{Q} = \hat{z}(4\pi/\lambda) \sin(\theta_0)$ be parallel to the surface normal, it is quite practical to obtain, for flat surfaces, an unambiguous separation of the specular reflection signal from all other scattering events.

Fig. 4.4.3.2(a) illustrates the specular reflectivity from the free nematic–air interface for the liquid crystal 4′-octyloxybiphenyl-4-carbonitrile (8OCB) 0.050 K above the nematic to smectic-A phase-transition temperature (Pershan & Als-Nielsen, 1984). The dashed line is the Fresnel reflection $R_F(\theta_0)$ in units of $\sin(\theta_0)/\sin(\theta_c)$,

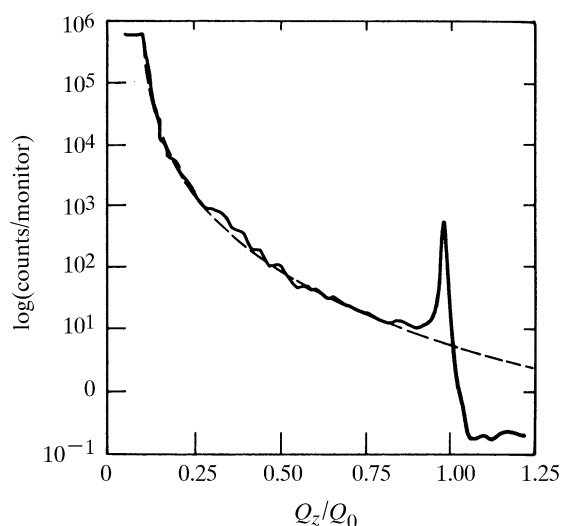


Fig. 4.4.3.2. Specular reflectivity of ~ 8 keV X-rays from the air–liquid interface of the nematic liquid crystal 8OCB 0.05 K above the nematic to smectic-A transition temperature. The dashed line is the Fresnel reflection law as described in the text.

where the peak at $\theta_c = 1.39^\circ$ corresponds to surface-induced smectic order in the nematic phase: *i.e.* the selection rule for specular reflection has been used to separate the specular reflection from the critical scattering from the bulk. Since the full width at half maximum is exactly equal to the reciprocal of the correlation length for critical fluctuations in the bulk, $2/\xi_{\parallel}$ at all temperatures from $T - T_{NA} \approx 0.006$ K up to values near to the nematic to isotropic transition, $T - T_{NA} \approx 3.0$ K, it is clear this is an example where the gravitationally induced long-range order in the surface position has induced mesomorphic order that has long-range correlations parallel to the surface. Along the surface normal, the correlations have only the same finite range as the bulk critical fluctuations. Studies on a number of other nematic (Gransbergen *et al.*, 1986; Ocko *et al.*, 1987) and isotropic surfaces (Ocko, Braslau *et al.*, 1986) indicate features that are specific to local structure of the surface.

4.4.4. Phases with in-plane order

Although the combination of optical microscopy and X-ray scattering studies on unoriented samples identified most of the mesomorphic phases, there remain a number of subtle features that were only discovered by spectra from well oriented samples (see the extensive references contained in Gray & Goodby, 1984). Nematic phases are sufficiently fluid that they are easily oriented by either external electric or magnetic fields, or surface boundary conditions, but similar alignment techniques are not generally successful for the more ordered phases because the combination of strains induced by thermal expansion and the enhanced elasticity that accompanies the order creates defects that do not easily anneal. Other defects that might have been formed during initial growth of the phase also become trapped and it is difficult to obtain well oriented samples by cooling from a higher-temperature aligned phase. Nevertheless, in some cases it has been possible to obtain crystalline-B samples with mosaic spreads of the order of a fraction of a degree by slowing cooling samples that were aligned in the nematic phase. In other cases, mesomorphic phases were obtained by heating and melting single crystals that were grown from solution (Benattar *et al.*, 1979; Leadbetter, Mazid & Malik, 1980).

Moncton & Pindak (1979) were the first to realize that X-ray scattering studies could be carried out on the freely suspended films that Friedel (1922) described in his classical treatise on liquid crystals. These samples, formed across a plane aperture (*i.e.* approximately 1 cm in diameter) in the same manner as soap bubbles, have mosaic spreads that are an order of magnitude smaller. The geometry is illustrated in Fig. 4.4.4.1(a). The substrate in which the aperture is cut can be glass (*e.g.* a microscope cover slip), steel or copper sheeting, *etc.* A small amount of the material, usually in the high-temperature region of the smectic-A phase, is spread around the outside of an aperture that is maintained at the necessary temperature, and a wiper is used to drag some of the material across the aperture. If a stable film is successfully drawn, it is detected optically by its finite reflectivity. In particular, against a dark background and with the proper illumination it is quite easy to detect the thinnest free films.

In contrast to conventional soap films that are stabilized by electrostatic effects, smectic films are stabilized by their own layer structure. Films as thin as two molecular layers can be drawn and studied for weeks (Young *et al.*, 1978). Thicker films of the order of thousands of layers can also be made and, with some experience in depositing the raw material around the aperture and the speed of drawing, it is possible to draw films of almost any desired thickness (Moncton *et al.*, 1982). For films thinner than approximately 20 to 30 molecular layers (*i.e.* 600 to 1000 Å), the thickness is determined from the reflected intensity of a small helium–neon laser. Since the

4.4. SCATTERING FROM MESOMORPHIC STRUCTURES

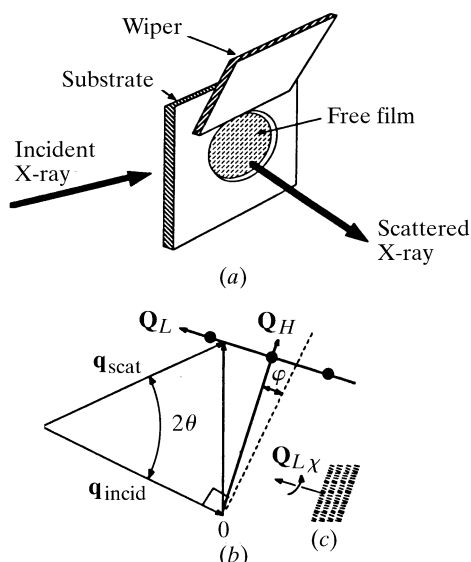


Fig. 4.4.4.1. (a) Schematic illustration of the geometry and (b) kinematics of X-ray scattering from a freely suspended smectic film. The insert (c) illustrates the orientation of the film in real space corresponding to the reciprocal-space kinematics in (b). If the angle $\varphi = \theta$, the film is oriented such that the scattering vector is parallel to the surface of the film, *i.e.* parallel to the smectic layers. A ' Q_L scan' is taken by simultaneous adjustment of φ and 2θ to keep $(4\pi/\lambda) \sin(\theta) \cos(\theta - \varphi) = (4\pi/\lambda) \sin(\theta_{100})$, where θ_{100} is the Bragg angle for the 100 reflection. The different in-plane Bragg reflections can be brought into the scattering plane by rotation of the film by the angle χ around the film normal.

reflected intensities for films of 2, 3, 4, 5, . . . layers are in the ratio of 4, 9, 16, 25, . . . , the measurement can be calibrated by drawing and measuring a reasonable number of thin films. The most straightforward method for thick films is to measure the ellipticity of the polarization induced in laser light transmitted through the film at an oblique angle (Collett, 1983; Collett *et al.*, 1985); however, a subtler method that makes use of the colours of white light reflected from the films is also practical (Sirota, Pershan, Sorensen & Collett, 1987). In certain circumstances, the thickness can also be measured using the X-ray scattering intensity in combination with one of the other methods.

Fig. 4.4.4.1 illustrates the scattering geometry used with these films. Although recent unpublished work has demonstrated the possibility of a reflection geometry (Sorensen, 1987), all of the X-ray scattering studies to be described here were performed in transmission. Since the in-plane molecular spacings are typically between 4 and 5 Å, while the layer spacing is closer to 30 Å, it is difficult to study the 00L peaks in this geometry.

Fig. 4.4.4.2 illustrates the difference between X-ray scattering spectra taken on a bulk crystalline-B sample of *N*-[4-(*n*-butyloxy)benzylidene]-4-*n*-octylaniline (4O.8) that was oriented in an external magnetic field while in the nematic phase and then cooled through the smectic-A phase into the crystalline-B phase (Aeppli *et al.*, 1981), and one taken on a thick freely suspended film of *N*-[4-(*n*-heptyloxy)benzylidene]-4-*n*-heptylaniline (7O.7) (Collett *et al.*, 1982, 1985). Note that the data for 7O.7 are plotted on a semi-logarithmic scale in order to display simultaneously both the Bragg peak and the thermal diffuse background. The scans are along the Q_L direction, at the appropriate value of Q_H to intersect the peaks associated with the intralayer periodicity. In both cases, the widths of the Bragg peaks are essentially determined by the sample mosaicity and as a result of the better alignment the ratio of the

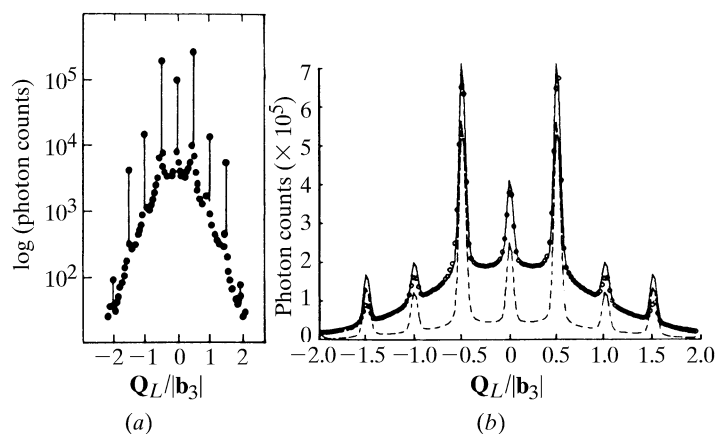


Fig. 4.4.4.2. Typical Q_L scans from the crystalline-B phases of (a) a free film of 7O.7, displayed on a logarithmic scale to illustrate the reduced level of the diffuse scattering relative to the Bragg reflection and (b) a bulk sample of 4O.8 oriented by a magnetic field.

thermal diffuse background to the Bragg peak is nearly an order of magnitude smaller for the free film sample.

4.4.4.1. Hexatic phases in two dimensions

The hexatic phase of matter was first proposed independently by Halperin & Nelson (Halperin & Nelson 1978; Nelson & Halperin 1979) and Young (Young, 1979) on the basis of theoretical studies of the melting process in two dimensions. Following work by Kosterlitz & Thouless (1973), they observed that since the interaction energy between pairs of dislocations in two dimensions decreases logarithmically with their separation, the enthalpy and the entropy terms in the free energy have the same functional dependence on the density of dislocations. It follows that the free-energy difference between the crystalline and hexatic phase has the form $\Delta F = \Delta H - T\Delta S \approx T_c S(\rho) - TS(\rho) = S(\rho)(T_c - T)$, where $S(\rho) \approx \rho \log(\rho)$ is the entropy as a function of the density of dislocations ρ and T_c is defined such that $T_c S(\rho)$ is the enthalpy. Since the prefactor of the enthalpy term is independent of temperature while that of the entropy term is linear, there will be a critical temperature, T_c , at which the sign of the free energy changes from positive to negative. For temperatures greater than T_c , the entropy term will dominate and the system will be unstable against the spontaneous generation of dislocations. When this happens, the two-dimensional crystal, with positional QLRO, but true long-range order in the orientation of neighbouring atoms, can melt into a new phase in which the positional order is short range, but for which there is QLRO in the orientation of the six neighbours surrounding any atom. The reciprocal-space structures for the two-dimensional crystal and hexatic phases are illustrated in Figs. 4.4.4.3(b) and (c), respectively. That of the two-dimensional solid consists of a hexagonal lattice of sharp rods (*i.e.* algebraic line shapes in the plane of the crystal). For a finite size sample, the reciprocal-space structure of the two-dimensional hexatic phase is a hexagonal lattice of diffuse rods and there are theoretical predictions for the temperature dependence of the in-plane line shapes (Aeppli & Bruinsma, 1984). If the sample were of infinite size, the QLRO of the orientation would spread the six spots continuously around a circular ring, and the pattern would be indistinguishable from that of a well correlated liquid, *i.e.* Fig. 4.4.4.3(a). The extent of the patterns along the rod corresponds to the molecular form factor. Figs. 4.4.4.3(a), (b) and (c) are drawn on the assumption that the molecules are normal to the two-

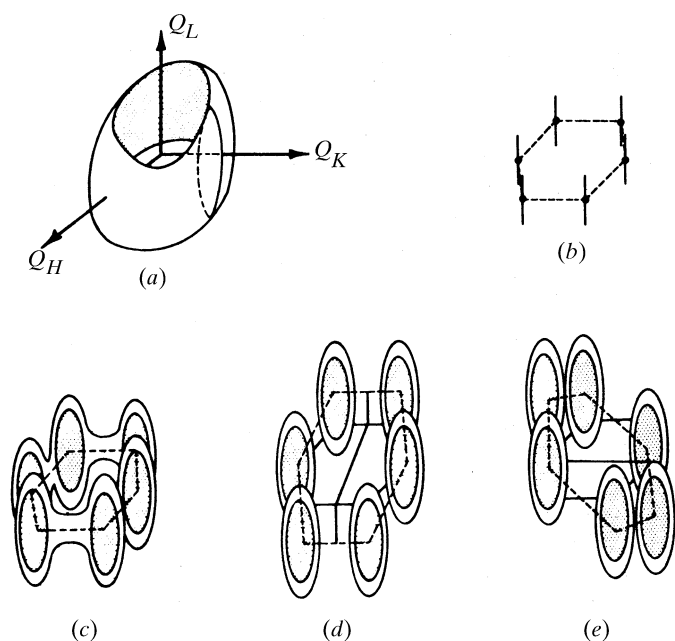


Fig. 4.4.4.3. Scattering intensities in reciprocal space from two-dimensional: (a) liquid; (b) crystal; (c) normal hexatic; and tilted hexatics in which the tilt is (d) towards the nearest neighbours as for the smectic-I or (e) between the nearest neighbours as for the smectic-F. The thin rods of scattering in (b) indicate the singular cusp for peaks with algebraic line shapes in the HK plane.

dimensional plane of the phase. If the molecules are tilted, the molecular form factor for long thin rod-like molecules will shift the intensity maxima as indicated in Figs. 4.4.4.3(d) and (e). The phase in which the molecules are normal to the two-dimensional plane is the two-dimensional *hexatic-B* phase. If the molecules tilt towards the position of their nearest neighbours (in real space), or in the direction that is between the lowest-order peaks in reciprocal space, the phase is the two-dimensional *smectic-I*, Fig. 4.4.4.3(d). The other tilted phase, for which the tilt direction is between the nearest neighbours in real space or in the direction of the lowest-order peaks in reciprocal space, is the *smectic-F*, Fig. 4.4.4.3(e).

Although theory (Halperin & Nelson, 1978; Nelson & Halperin, 1979; Young, 1979) predicts that the two-dimensional crystal can melt into a hexatic phase, it does not say that it must happen, and the crystal can melt directly into a two-dimensional liquid phase. Obviously, the hexatic phases will also melt into a two-dimensional liquid phase. Fig. 4.4.4.3(a) illustrates the reciprocal-space structure for the two-dimensional liquid in which the molecules are normal to the two-dimensional surface. Since the longitudinal (*i.e.* radial) width of the hexatic spot could be similar to the width that might be expected in a well correlated fluid, the direct X-ray proof of the transition from the hexatic-B to the normal liquid requires a hexatic sample in which the domains are sufficiently large that the sample is not a two-dimensional powder. On the other hand, the elastic constants must be sufficiently large that the QLRO does not smear the six spots into a circle. The radial line shape of the powder pattern of the hexatic-B phase can also be subtly different from that of the liquid and this is another possible way that X-ray scattering can detect melting of the hexatic-B phase (Aeppli & Bruinsma, 1984).

Changes that occur on the melting of the tilted hexatics, *i.e.* smectic-F and smectic-I, are usually easier to detect and this will be discussed in more detail below. On the other hand, there is a fundamental theoretical problem concerning the way of understanding the melting of the tilted hexatics. These phases actually

have the same symmetry as the two-dimensional tilted fluid phase, *i.e.* the smectic-C. In two dimensions they all have QLRO in the tilt orientation, and since the simplest phenomenological argument says that there is a linear coupling between the tilt order and the near-neighbour positional order (Nelson & Halperin, 1980; Bruinsma & Nelson, 1981), it follows that the QLRO of the smectic-C tilt should induce QLRO in the near-neighbour positional order. Thus, by the usual arguments, if there is to be a phase transition between the smectic-C and one of the tilted hexatic phases, the transition must be a first-order transition (Landau & Lifshitz, 1958). This is analogous to the three-dimensional liquid-to-vapour transition which is first order up to a critical point, and beyond the critical point there is no real phase transition.

4.4.4.2. Hexatic phases in three dimensions

Based on both this theory and the various X-ray scattering patterns that had been reported in the literature (Gray & Goodby, 1984), Litster & Birgeneau (Birgeneau & Litster, 1978) suggested that some of the three-dimensional systems that were previously identified as mesomorphic were actually three-dimensional hexatic systems. They observed that it is not theoretically consistent to propose that the smectic phases are layers of two-dimensional crystals randomly displaced with respect to each other since, in thermal equilibrium, the interactions between layers of two-dimensional crystals must necessarily cause the layers to lock together to form a three-dimensional crystal.* On the other hand, if the layers were two-dimensional hexatics, then the interactions would have the effect of changing the QLRO of the hexagonal distribution of neighbours into the true long-range-order orientational distribution of the three-dimensional hexatic. In addition, interactions between layers in the three-dimensional hexatics can also result in interlayer correlations that would sharpen the width of the diffuse peaks in the reciprocal-space direction along the layer normal.

4.4.4.2.1. Hexatic-B

Although Leadbetter, Frost & Mazid (1979) had remarked on the different types of X-ray structures that were observed in materials identified as 'smectic-B', the first proof for the existence of the hexatic-B phase of matter was the experiment by Pindak *et al.* (1981) on thick freely suspended films of the liquid crystal *n*-hexyl 4'-pentyloxybiphenyl-4-carboxylate (65OBC). A second study on free films of the liquid crystal *n*-butyl 4'-*n*-hexyloxybiphenyl-4-carboxylate (46OBC) demonstrated that, as the hexatic-B melts into the smectic-A phase, the position and the in-plane width of the X-ray scattering peaks varied continuously. In particular, the in-plane correlation length evolved continuously from 160 Å, nearly 10 K below the hexatic to smectic-A transition, to only 17 Å, a few degrees above. Similar behaviour was also observed in a film only two layers thick (Davey *et al.*, 1984). Since the observed width of the peak along the layer normal corresponded to the molecular form factor, these systems have negligible interlayer correlations.

4.4.4.2.2. Smectic-F, smectic-I

In contrast to the hexatic-B phase, the principal reciprocal-space features of the smectic-F phase were clearly determined before the theoretical work that proposed the hexatic phase. Demus *et al.* (1971) identified a new phase in one material, and subsequent X-ray studies by Leadbetter and co-workers (Leadbetter, Mazid & Richardson, 1980; Leadbetter, Gaughan *et al.*, 1979; Gane &

* Prior to the paper by Birgeneau & Litster, it was commonly believed that some of the smectic phases consisted of uncorrelated stacks of two-dimensional crystals.

4.4. SCATTERING FROM MESOMORPHIC STRUCTURES

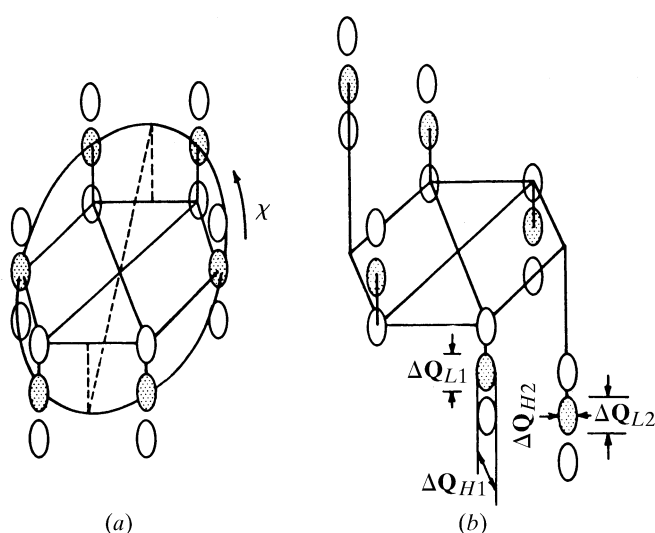


Fig. 4.4.4.4. Scattering intensities in reciprocal space from three-dimensional tilted hexatic phases: (a) the smectic-I and (b) the smectic-F. The variation of the intensity along the Q_L direction indicates interlayer correlations that are absent in Figs. 4.4.4.1(d) and (e). The peak widths $\Delta Q_{L1,2}$ and $\Delta Q_{H1,2}$ correspond to the four inequivalent widths in the smectic-F phase. Similar inequivalent widths exist for the smectic-I phase. The circle through the shaded points in (a) indicates the reciprocal-space scan that directly measures the hexatic order. A similar scan in the smectic-C phase would have intensity independent of χ .

Leadbetter, 1981) and by Benattar and co-workers (Benattar *et al.*, 1978, 1980, 1983; Guillon *et al.*, 1986) showed it to have the reciprocal-space structure illustrated in Fig. 4.4.4.4(b). There are interlayer correlations in the three-dimensional smectic-F phases, and as a consequence the reciprocal-space structure has maxima along the diffuse rods. Benattar *et al.* (1979) obtained monodomain smectic-F samples of the liquid crystal N,N' -(1,4-phenylenedimethylene)bis(4-*n*-pentylaniline) by melting a single crystal that was previously precipitated from solution. One of the more surprising results of this work was the demonstration that the near-neighbour packing was very close to what would be expected from a model in which rigid closely packed rods were simply tilted away from the layer normal. In view of the facts that the molecules are clearly not cylindrical, and that the molecular tilt indicates that the macroscopic symmetry has been broken, it would have been reasonable to expect significant deviations from local hexagonal symmetry when the system is viewed along the molecular axis. The fact that this is not the case indicates that this phase has a considerable amount of rotational disorder around the long axis of the molecules.

Other important features of the smectic-F phase are, firstly, that the local molecular packing is identical to that of the tilted crystalline-G phase (Benattar *et al.*, 1979; Sirota *et al.*, 1985; Guillon *et al.*, 1986). Secondly, there is considerable temperature dependence of the widths of the various diffuse peaks. Fig. 4.4.4.4(b) indicates the four inequivalent line widths that Sirota and co-workers measured in freely suspended films of the liquid crystal N -[4-(*n*-heptyloxy)benzylidene]-4-*n*-heptyl aniline (70.7). Parenthetically, bulk samples of this material do not have a smectic-F phase; however, the smectic-F is observed in freely suspended films as thick as ~ 200 layers. Fig. 4.4.4.5 illustrates the thickness-temperature phase diagram of 70.7 between 325 and 342 K (Sirota *et al.*, 1985; Sirota, Pershan & Deutsch, 1987). Bulk samples and thick films have a first-order transition from the crystalline-B to the smectic-C at 342 K. Thinner films indicate a surface phase above

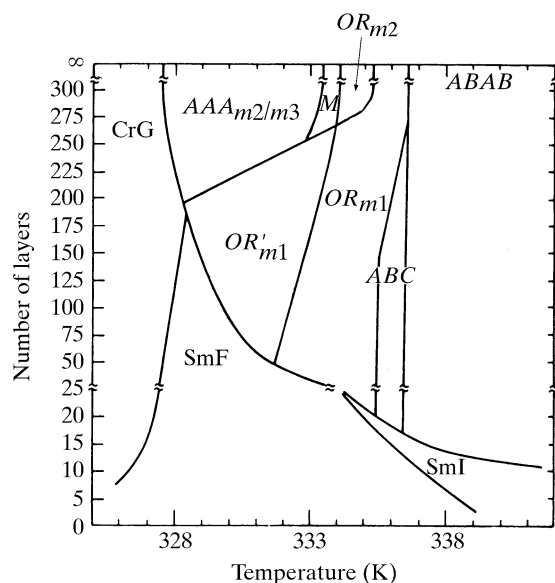


Fig. 4.4.4.5. The phase diagram for free films of 70.7 as a function of thickness and temperature. The phases *ABAB*, *AAA*, *OR_{m1}*, *OR_{m2}*, *OR'_{m1}*, *M* and *ABAB* are all crystalline-B with varying interlayer stacking, or long-wavelength modulations; *CrG*, *SmF* and *SmI* are crystalline-G, smectic-F and smectic-I, respectively (Sirota *et al.*, 1985; Sirota, Pershan & Deutsch, 1987; Sirota, Pershan, Sorensen & Collett, 1987).

342 K that will be discussed below. Furthermore, although there is a strong temperature dependence of the widths of the diffuse scattering peaks, the widths are independent of film thickness. This demonstrates that, although the free film boundary conditions have stabilized the smectic-F phase, the properties of the phase are not affected by the boundaries. Finally, the fact that the widths ΔQ_{L1} and ΔQ_{L2} along the L direction and ΔQ_{H1} and ΔQ_{H2} along the in-plane directions are not equal indicates that the correlations are very anisotropic (Brock *et al.*, 1986; Sirota *et al.*, 1985). We will discuss one possible model for these properties after presenting other data on thick films of 70.7. From the fact that the positions of the intensity maxima for the diffuse spots of the smectic-F phase of 70.7 correspond exactly to the positions of the Bragg peaks in the crystalline-G phase, we learn that the local molecular packing must be identical in the two phases. The major difference between the crystalline-G and the tilted hexatic smectic-F phase is that, in the latter, defects destroy the long-range positional order of the former (Benattar *et al.*, 1979; Sirota *et al.*, 1985). Although this is consistent with the existing theoretical model that attributes hexatic order to a proliferation of unbounded dislocations, it is not obvious that the proliferation is attributable to the same Kosterlitz-Thouless mechanism that Halperin & Nelson and Young discussed for the transition from the two-dimensional crystal to the hexatic phase. We will say more on this point below.

The only identified difference between the two tilted hexatic phases, the smectic-F and the smectic-I, is the direction of the molecular tilt relative to the near-neighbour positions. For the smectic-I, the molecules tilt towards one of the near neighbours, while for the smectic-F they tilt between the neighbours (Gane & Leadbetter, 1983). There are a number of systems that have both smectic-I and smectic-F phases, and in all cases of which we are aware the smectic-I is the higher-temperature phase (Gray & Goodby, 1984; Sirota *et al.*, 1985; Sirota, Pershan, Sorensen & Collett, 1987).

Optical studies of freely suspended films of materials in the nO_m series indicated tilted surface phases at temperatures for which the bulk had uniaxial phases (Farber, 1985). As mentioned above,

4. DIFFUSE SCATTERING AND RELATED TOPICS

X-ray scattering studies of 70.7 demonstrated that the smectic-F phase set in for a narrow temperature range in films as thick as 180 layers, and that the temperature range increases with decreasing layer number. For films of the order of 25 layers thick, the smectic-I phase is observed at approximately 334 K, and with decreasing thickness the temperature range for this phase also increases. Below approximately 10 to 15 layers, the smectic-I phase extends up to ~ 342 K where bulk samples undergo a first-order transition from the crystalline-B to the smectic-C phase. Synchrotron X-ray scattering experiments show that, in thin films (five layers for example), the homogeneous smectic-I film undergoes a first-order transition to one in which the two surface layers are smectic-I and the three interior layers are smectic-C (Sirota *et al.*, 1985; Sirota, Pershan, Sorensen & Collett, 1987). The fact that two phases with the same symmetry can coexist in this manner tells us that in this material there is some important microscopic difference between them. This is reaffirmed by the fact that the phase transition from the surface smectic-I to the homogeneous smectic-C phase has been observed to be first order (Sorensen *et al.*, 1987).

In contrast to 70.7, Birgeneau and co-workers found that in racemic 4-(2-methylbutyl)phenyl 4'-octyloxybiphenyl-4-carboxylate (8OSI) (Brock *et al.*, 1986), the X-ray structure of the smectic-I phase evolves continuously into that of the smectic-C. By applying a magnetic field to a thick freely suspended sample, Brock *et al.* were able to obtain a large monodomain sample. They measured the X-ray scattering intensity around the circle in the reciprocal-space plane shown in Fig. 4.4.4.4(b) that passes through the peaks. For higher temperatures, when the sample is in the smectic-C phase, the intensity is essentially constant around the circle; however, on cooling, it gradually condenses into six peaks, separated by 60° . The data were analysed by expressing the intensity as a Fourier series of the form

$$S(\chi) = I_0 \left[\frac{1}{2} + \sum_{n=1}^{\infty} C_{6n} \cos 6n(90^\circ - \chi) \right] + I_B,$$

where I_0 fixes the absolute intensity and I_B fixes the background. The temperature variation of the coefficients scaled according to the relation $C_{6n} = C_6^{\sigma n}$ where the empirical relation $\sigma_n = 2.6(n-1)$ is in good agreement with a theoretical form predicted by Aharony *et al.* (1986). The only other system in which this type of measurement has been made was the smectic-C phase of 70.7 (Collett, 1983). In that case, the intensity around the circle was constant, indicating the absence of any tilt-induced bond orientational order (Aharony *et al.*, 1986).

It would appear that the near-neighbour molecular packing of the smectic-I and the crystalline-J phases is the same, in just the same way as for the packing of the smectic-F and the crystalline-G phases. The four smectic-I widths analogous to those illustrated in Fig. 4.4.4.4(a) are, like that of the smectic-F, both anisotropic and temperature dependent (Sirota *et al.*, 1985; Sirota, Pershan, Sorensen & Collett, 1987; Brock *et al.*, 1986; Benattar *et al.*, 1979).

4.4.4.3. Crystalline phases with molecular rotation

4.4.4.3.1. Crystal-B

Recognition of the distinction between the hexatic-B and crystalline-B phases provided one of the more important keys to understanding the ordered mesomorphic phases. There are a number of distinct phases called crystalline-B that are all true three-dimensional crystals, with resolution-limited Bragg peaks (Moncton & Pindak, 1979; Aeppli *et al.*, 1981). The feature common to them all is that the average molecular orientation is normal to the layers, and within each layer the molecules are distributed on a triangular lattice. In view of the 'blade-like' shape of the molecule, the hexagonal site symmetry implies that the

molecules must be rotating rapidly (Levelut & Lambert, 1971; Levelut, 1976; Richardson *et al.*, 1978). We have previously remarked that this apparent rotational motion characterizes all of the phases listed in Table 4.4.1.1 except for the crystalline-E, -H and -K. In the most common crystalline-B phase, adjacent layers have ABAB-type stacking (Leadbetter, Gaughan *et al.*, 1979; Leadbetter, Mazid & Kelly, 1979). High-resolution studies on well oriented samples show that in addition to the Bragg peaks the crystalline-B phases have rods of relatively intense diffuse scattering distributed along the 10L Bragg peaks (Moncton & Pindak, 1979; Aeppli *et al.*, 1981). The widths of these rods in the reciprocal-space direction, parallel to the layers, are very sharp, and without a high-resolution spectrometer their widths would appear to be resolution limited. In contrast, along the reciprocal-space direction normal to the layers, their structure corresponds to the molecular form factor.

If the intensity of the diffuse scattering can be represented as proportional to $(\mathbf{Q} \cdot \mathbf{u})^2$, where \mathbf{u} describes the molecular displacement, the fact that there is no rod of diffuse scattering through the 00L peaks indicates that the rods through the 10L peaks originate from random disorder in 'sliding' displacements of adjacent layers. It is likely that these displacements are thermally excited phonon vibrations; however, we cannot rule out some sort of non-thermal static defect structure. In any event, assuming this diffuse scattering originates in a thermal vibration for which adjacent layers slide over one another with some amplitude $\langle \mathbf{u}^2 \rangle^{1/2}$, and assuming strong coupling between this shearing motion and the molecular tilt, we can define an angle $\varphi = \tan^{-1}(\langle \mathbf{u}^2 \rangle^{1/2}/d)$, where d is the layer thickness. The observed diffuse intensity corresponds to angles φ between 3 and 6° (Aeppli *et al.*, 1981).

Leadbetter and co-workers demonstrated that in the $nO.m$ series various molecules undergo a series of restacking transitions and that crystalline-B phases exist with ABC and AAA stacking as well as the more common ABAB (Leadbetter, Mazid & Richardson 1980; Leadbetter, Mazid & Kelly, 1979). Subsequent high-resolution studies on thick freely suspended films revealed that the restacking transitions were actually subtler, and in 70.7, for example, on cooling the hexagonal ABAB phase one observes an orthorhombic and then a monoclinic phase before the hexagonal AAA (Collett *et al.*, 1982, 1985). Furthermore, the first transition from the hexagonal ABAB to the monoclinic phase is accompanied by the appearance of a relatively long wavelength modulation within the plane of the layers. The polarization of this modulation is along the layer normal, or orthogonal to the polarization of the displacements that gave rise to the rods of thermal diffuse scattering (Gane & Leadbetter, 1983).

It is also interesting to note that the AAA simple hexagonal structure does not seem to have been observed outside liquid-crystalline materials and, were it not for the fact that the crystalline-B hexagonal AAA is always accompanied by long wavelength modulations, it would be the only case of which we are aware.

Figs. 4.4.4.6(a) and (b) illustrate the reciprocal-space positions of the Bragg peaks (dark dots) and modulation-induced side bands (open circles) for the unmodulated hexagonal ABAB and the modulated orthorhombic phase (Collett *et al.*, 1984). For convenience, we only display one 60° sector. Hirth *et al.* (1984) explained how both the reciprocal-space structure and the modulation of the orthorhombic phase could result from an ordered array of partial dislocations. They were not, however, able to provide a specific model for the microscopic driving force for the transition. Sirota, Pershan & Deutsch (1987) proposed a variation of the Hirth model in which the dislocations pair up to form a wall of dislocation dipoles such that within the wall the local molecular packing is essentially identical to the packing in the crystalline-G phase that appears at temperatures just below the crystalline-B phase. This model explains: (1) the macroscopic symmetry of the

4.4. SCATTERING FROM MESOMORPHIC STRUCTURES

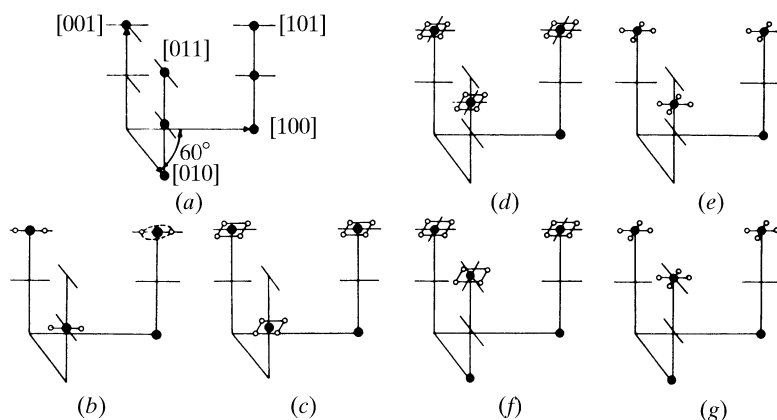


Fig. 4.4.4.6. Location of the Bragg peaks in one 60° section of reciprocal space for the three-dimensional crystalline-B phases observed in thick films of 7O.7. (a) The normal hexagonal crystalline-B phase with *ABAB* stacking. (b) The one-dimensional modulated phase with orthorhombic symmetry. The closed circles are the principal Bragg peaks and the open circles indicate side bands associated with the long-wavelength modulation. (c) The two-dimensional modulated phase with orthorhombic symmetry. Only the lowest-order side bands are shown. They are situated on the corners of squares surrounding the Bragg peak. The squares are oriented as shown and the amplitude of the square diagonal is equal to the distance between the two side bands illustrated in (b). (d) The two-dimensional modulated phase with monoclinic symmetry. Note that the *L* position of one of the peaks has shifted relative to (c). (e) A two-dimensional modulated phase with orthorhombic symmetry that is only observed on heating the quenched phase illustrated in (g). (f) The two-dimensional modulated phase with hexagonal symmetry and *AAA* layer stacking. (g) A two-dimensional hexagonal phase with *AAA* layer stacking that is only observed on rapid cooling from the phase shown in (c).

phase; (2) the period of the modulation; (3) the polarization of the modulation; and (4) the size of the observed deviations of the reciprocal-space structure from the hexagonal symmetry of the *ABAB* phase and suggests a microscopic driving mechanism that we will discuss below.

On further cooling, there is a first-order transition in which the one-dimensional modulation that appeared at the transition to orthorhombic symmetry is replaced by a two-dimensional modulation as shown in Fig. 4.4.4.6(c). On further cooling, there is another first-order transition in which the positions of the principal Bragg spots change from having orthorhombic to monoclinic symmetry as illustrated in Fig. 4.4.4.6(d). On further cooling, the Bragg peaks shift continually until there is one more first-order transition to a phase with hexagonal *AAA* positions as illustrated in Fig. 4.4.4.6(f). On further cooling, the *AAA* symmetry remains unchanged, and the modulation period is only slightly dependent on temperature, but the modulation amplitude increases dramatically. Eventually, as indicated in the phase diagram shown in Fig. 4.4.4.5, the system undergoes another first-order transition to the tilted crystalline-G phase. The patterns in Figs. 4.4.4.6(e) and (g) are observed by rapid quenching from the temperatures at which the patterns in Fig. 4.4.4.6(b) are observed.

Although there is not yet an established theoretical explanation for the origin of the 'restacking-modulation' effects, there are a number of experimental facts that we can summarize, and which indicate a probable direction for future research. Firstly, if one ignores the long wavelength modulation, the hexagonal *ABAB* phase is the only phase in the diagram for 7O.7 for which there are two molecules per unit cell. There must be some basic molecular effect that determines this particular coupling between every other layer. In addition, it is particularly interesting that it only manifests itself for a small temperature range and then vanishes as the sample is cooled. Secondly, any explanation for the driving force of the restacking transition must also explain the modulations that accompany it. In particular, unless one cools rapidly, the same modulation structures with the same amplitudes always appear at the same temperature, regardless of the sample history, *i.e.* whether heating or cooling. No significant hysteresis is observed and Sirota argued that the structures are in thermal equilibrium.

There are a number of physical systems for which the development of long-wavelength modulations is understood, and

in each case they are the result of two or more competing interaction energies that cannot be simultaneously minimized (Blinic & Levanyuk, 1986; Safinya, Varady *et al.*, 1986; Lubensky & Ingersent, 1986; Winkor & Clarke, 1986; Moncton *et al.*, 1981; Fleming *et al.*, 1980; Villain, 1980; Frank & van der Merwe, 1949; Bak *et al.*, 1979; Pokrovsky & Talapov, 1979). The easiest to visualize is epitaxial growth of one crystalline phase on the surface of another when the two lattice vectors are slightly incommensurate. The first atomic row of adsorbate molecules can be positioned to minimize the attractive interactions with the substrate. This is slightly more difficult for the second row, since the distance that minimizes the interaction energy between the first and second rows of adsorbate molecules is not necessarily the same as the distance that would minimize the interaction energy between the first row and the substrate. As more and more rows are added, the energy price of this incommensurability builds up, and one possible configuration that minimizes the global energy is a modulated structure.

In all known cases, the very existence of modulated structures implies that there must be competing interactions, and the only real question about the modulated structures in the crystalline-B phases is the identification of the competing interactions. It appears that one of the more likely possibilities is the difficulty in packing the 7O.7 molecules within a triangular lattice while simultaneously optimizing the area per molecule of the alkane tails and the conjugated rings in the core (Carlson & Sethna, 1987; Sadoc & Charvolin, 1986). Typically, the mean cross-sectional area for a straight alkane in the all-*trans* configuration is between 18 and 19 Å², while the mean area per molecule in the crystalline-B phase is closer to 24 Å². While these two could be reconciled by assuming that the alkanes are tilted with respect to the conjugated core, there is no reason why the angle that reconciles the two should also be the same angle that minimizes the internal energy of the molecule. Even if it were the correct angle at some temperature by accident, the average area per chain is certainly temperature dependent. Even without attempting to include the rotational dynamics that are necessary to understanding the axial site symmetry, it is obvious that there can be a conflict in the packing requirements of the two different parts of the molecule.

A possible explanation of these various structures might be as follows: at high temperatures, both the alkane chain, as well as the

4. DIFFUSE SCATTERING AND RELATED TOPICS

other degrees of freedom, have considerable thermal motions that make it possible for the conflicting packing requirements to be simultaneously reconciled by one or another compromise. On the other hand, with decreasing temperature, some of the thermal motions become frozen out, and the energy cost of the reconciliation that was possible at higher temperatures becomes too great. At this point, the system must find another solution, and the various modulated phases represent the different compromises. Finally, all of the compromises involving inhomogeneities, like the modulations or grain boundaries, become impossible and the system transforms into a homogeneous crystalline-G phase.

If this type of argument could be made more specific, it would also provide a possible explanation for the molecular origin of the three-dimensional hexatic phases. The original suggestion for the existence of hexatic phases in two dimensions was based on the fact that the interaction energy between dislocations in two dimensions was logarithmic, such that the entropy and the enthalpy had the same functional dependence on the density of dislocations. This gave rise to the observation that above a certain temperature two-dimensional crystals would be unstable against thermally generated dislocations. Although Litster and Birgeneau's suggestion that some of the observed smectic phases might be stacks of two-dimensional hexatics is certainly correct, it is not necessary that the observed three-dimensional hexatics originate from entropy-driven thermally excited dislocations. For example, the temperature–layer-number phase diagram for 7O.7 that is shown in Fig. 4.4.4.5 has the interesting property that the temperature region over which the tilted hexatic phases exist in thin films is almost the same as the temperature region for which the modulated phases exist in thick films and in bulk samples.

From the fact that molecules in the *nO.m* series that only differ by one or two $-\text{CH}_2-$ groups have different sequences of mesomorphic phases, we learn that within any one molecule the difference in chemical potentials between the different mesomorphic phases must be very small (Leadbetter, Mazid & Kelly, 1979; Doucet & Levelut, 1977; Leadbetter, Frost & Mazid, 1979; Leadbetter, Mazid & Richardson, 1980; Smith *et al.*, 1973; Smith & Garland, 1973). For example, although in 7O.7 the smectic-F phase is only observed in finite-thickness films, both 5O.6 and 9O.4 have smectic-F phase in bulk. Thus, in bulk 7O.7 the chemical potential for the smectic-F phase must be only slightly larger than that of the modulated crystalline-B phases, and the effect of the surfaces must be sufficient to reverse the order in samples of finite thickness.

As far as the appearance of the smectic-F phase in 7O.7 is concerned, it is well known that the interaction energy between dislocation pairs is very different near a free surface from that in the bulk (Pershan, 1974; Pershan & Prost, 1975). The origin of this is that the elastic properties of the surface will usually cause the stress field of a dislocation near to the surface either to vanish or to be considerably smaller than it would in the bulk. Since the interaction energy between dislocations depends on this stress field, the surface significantly modifies the dislocation–dislocation interaction. This is a long-range effect, and it would not be surprising if the interactions that stabilized the dislocation arrays to produce the long-wavelength modulations in the thick samples were sufficiently weaker in the samples of finite thickness that the dislocation arrays are disordered. Alternatively, there is evidence that specific surface interactions favour a finite molecular tilt at temperatures where the bulk phases are uniaxial (Farber, 1985). Incommensurability between the period of the tilted surface molecules and the crystalline-B phases below the surface would increase the density of dislocations, and this would also modify the dislocation–dislocation interactions in the bulk.

Sirota *et al.* (1985) and Sirota, Pershan, Sorensen & Collett (1987) demonstrated that, while the correlation lengths of the smectic-F phase have a significant temperature dependence, the

lengths are independent of film thickness, and this supports the argument that although the effects of the surface are important in stabilizing the smectic-F phase in 7O.7, once the phase is established it is essentially no different from the smectic-F phases observed in bulk samples of other materials. Brock *et al.* (1986) observed anisotropies in the correlation lengths of thick samples of 8OSI that are similar to those observed by Sirota.

These observations motivate the hypothesis that the dislocation densities in the smectic-F phases are determined by the same incommensurability that gives rise to the modulated crystalline-B structures. Although all of the experimental evidence supporting this hypothesis was obtained from the smectic-F tilted hexatic phase, there is no reason why this speculation could not apply to both the tilted smectic-I and the untilted hexatic-B phase.

4.4.4.3.2. Crystal-G, crystal-J

The crystalline-G and crystalline-J phases are the ordered versions of the smectic-F and smectic-I phases, respectively. The positions of the principal peaks illustrated in Fig. 4.4.4.4 for the smectic-F(I) are identical to the positions in the smectic-G(J) phase if small thermal shifts are discounted. In both the hexatic and the crystalline phases, the molecules are tilted with respect to the layer normals by approximately 25 to 30° with nearly hexagonal packing around the tilted axis (Doucet & Levelut, 1977; Levelut *et al.*, 1974; Levelut, 1976; Leadbetter, Mazid & Kelly, 1979; Sirota, Pershan, Sorensen & Collett, 1987). The interlayer molecular packing appears to be end to end, in an AAA type of stacking (Benattar *et al.*, 1983; Benattar *et al.*, 1981; Levelut, 1976; Gane *et al.*, 1983). There is only one molecule per unit cell and there is no evidence for the long-wavelength modulations that are so prevalent in the crystalline-B phase that is the next higher temperature phase above the crystalline-G in 7O.7.

4.4.4.4. Crystalline phases with herringbone packing

4.4.4.4.1. Crystal-E

Fig. 4.4.4.7 illustrates the intralayer molecular packing proposed for the crystalline-E phase (Levelut, 1976; Doucet, 1979; Levelut *et al.*, 1974; Doucet *et al.*, 1975; Leadbetter *et al.*, 1976; Richardson *et al.*, 1978; Leadbetter, Frost, Gaughan & Mazid, 1979; Leadbetter, Frost & Mazid, 1979). The molecules are, on average, normal to the

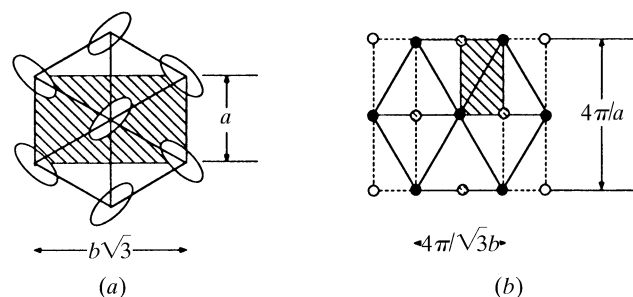


Fig. 4.4.4.7. (a) The 'herringbone' stacking suggested for the crystalline-E phase in which molecular rotation is partially restricted. The primitive rectangular unit cell containing two molecules is illustrated by the shaded region. The lattice has rectangular symmetry and $a \neq b$. (b) The position of the Bragg peaks in the plane in reciprocal space that is parallel to the layers. The dark circles indicate the principal Bragg peaks that would be the only ones present if all molecules were equivalent. The open circles indicate additional peaks that are observed for the model illustrated in (a). The cross-hatched circles indicate peaks that are missing because of the glide plane in (a).

4.4. SCATTERING FROM MESOMORPHIC STRUCTURES

layers; however, from the optical birefringence it is apparent that the site symmetry is not uniaxial. X-ray diffraction studies on single crystals by Doucet and co-workers demonstrated that the biaxiality was not attributable to molecular tilt and subsequent work by a number of others resulted in the arrangement shown in Fig. 4.4.4.7(a). The most important distinguishing reciprocal-space feature associated with the intralayer 'herringbone' packing is the appearance of Bragg peaks at $\sin(\theta)$ equal to $\sqrt{7}/2$ times the value for the lowest-order in-plane Bragg peak for the triangular lattice (Pindak *et al.*, 1981). These are illustrated by the open circles in Fig. 4.4.4.7(b). The shaded circles correspond to peaks that are missing because of the glide plane that relates the two molecules in the rectangular cell.

Leadbetter, Mazid & Malik (1980) carried out detailed studies on both the crystalline-E phase of isobutyl 4-(4-phenylbenzylidene-amino)cinnamate (IBPBAC) and the crystalline phase immediately below the crystalline-E phase. Partially ordered samples of the crystalline-E phase were obtained by melting the lower-temperature crystalline phase. Although the data for the crystalline-E phase left some ambiguity, they argued that the phase they were studying might well have had molecular tilts of the order of 5 or 6°. This is an important distinction, since the crystalline-H and crystalline-J phases are essentially tilted versions of the crystalline-E. Thus, one important symmetry difference that might distinguish the crystalline-E from the others is the presence of a mirror plane parallel to the layers. In view of the low symmetry of the individual molecules, the existence of such a mirror plane would imply residual molecular motions. In fact, using neutron diffraction Leadbetter *et al.* (1976) demonstrated for a different liquid crystal that, even though the site symmetry is not axially symmetric, there is considerable residual rotational motion in the crystalline-E phase about the long axis of the molecules. Since the in-plane spacing is too small for neighbouring molecules to be rotating independently of each other, they proposed what might be interpreted as large partially hindered rotations.

4.4.4.4.2. Crystal-H, crystal-K

The crystalline-H and crystalline-K phases are tilted versions of the crystalline-E. The crystalline-H is tilted in the direction between the near neighbours, with the convenient mnemonic that on cooling the sequence of phases with the same relative orientation of tilt to near-neighbour position is F → G → H. Similarly, the tilt direction for the crystalline-K phase is similar to that of the smectic-I and crystalline-J so that the expected phase sequence on cooling might be I → J → K. In fact, both of these sequences are only intended to indicate the progression in lower symmetry; the actual transitions vary from material to material.

4.4.5. Discotic phases

In contrast to the long thin rod-like molecules that formed most of the other phases discussed in this chapter, the discotic phases are formed by molecules that are more disc-like [see Fig. 4.4.1.3(f), for example]. There was evidence that mesomorphic phases were formed from disc-like molecules as far back as 1960 (Brooks & Taylor, 1968); however, the first identification of a discotic phase was by Chandrasekhar *et al.* (1977) with benzenehexyl hexa-*n*-alkanoate compounds. Disc-like molecules can form either a fluid nematic phase in which the disc normals are aligned, without any particular long-range order at the molecular centre of mass, or more-ordered 'columnar' (Helfrich, 1979) or 'discotic' (Billard *et al.*, 1981) phases in which the molecular positions are correlated such that the discs stack on top of one another to form columns. Some of the literature designates this nematic phase as N_D to distinguish it from the phase formed by 'rod-like' molecules

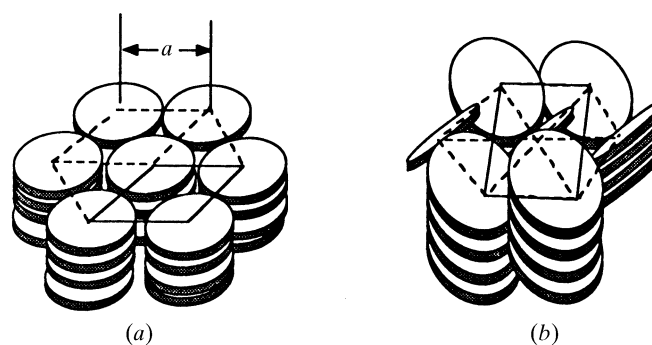


Fig. 4.4.5.1. Schematic illustration of the molecular stacking for the discotic (a) D_2 and (b) D_1 phases. In neither of these two phases is there any indication of long-range positional order along the columns. The hexagonal symmetry of the D_1 phase is broken by 'herringbone-like' correlations in the molecular tilt from column to column.

(Destrade *et al.*, 1983). In the same way that the appearance of layers characterizes order in smectic phases, the order for the discotic phases is characterized by the appearance of columns. Chandrasekhar (1982, 1983) and Destrade *et al.* (1983) have reviewed this area and have summarized the several notations for various phases that appear in the literature. Levelut (1983) has also written a review and presented a table listing the space groups for columnar phases formed by 18 different molecules. Unfortunately, it is not absolutely clear which of these are mesomorphic phases and which are crystals with true long-range positional order.

Fig. 4.4.5.1 illustrates the molecular packing in two of the well identified discotic phases that are designated as D_1 and D_2 (Chandrasekhar, 1982). The phase D_2 consists of a hexagonal array of columns for which there is no intracolumnar order. The system is uniaxial and, as originally proposed, the molecular normals were supposed to be along the column axis. However, recent X-ray scattering studies on oriented free-standing fibres of the D_2 phase of triphenylene hexa-*n*-dodecanoate indicate that the molecules are tilted with respect to the layer normal (Safinya *et al.*, 1985, 1984). The D_1 phase is definitely a tilted phase, and consequently the columns are packed in a rectangular cell. According to Safinya *et al.*, the D_1 to D_2 transition corresponds to an order-disorder transition in which the molecular tilt orientation is ordered about the column axis in the D_1 phase and disordered in the D_2 phase. The reciprocal-space structure of the D_1 phase is similar to that of the crystalline-E phase shown in Fig. 4.4.4.7(b).

Other discotic phases that have been proposed would have the molecules arranged periodically along the column, but disordered between columns. This does not seem physically realistic since it is well known that thermal fluctuations rule out the possibility of a one-dimensional periodic structure even more strongly than for the two-dimensional lattice that was discussed above (Landau, 1965; Peierls, 1934). On the other hand, in the absence of either more high-resolution studies on oriented fibres or further theoretical studies, we prefer not to speculate on the variety of possible true discotic or discotic-like crystalline phases that might exist. This is a subject for future research.

4.4.6. Other phases

We have deliberately chosen not to discuss the properties of the cholesteric phase in this chapter because the length scales that characterize the long-range order are of the order of micrometres and are more easily studied by optical scattering than by X-rays (De Gennes, 1974; De Vries, 1951). Nematic phases formed from chiral